The Origin of Base Catalysis in the •OH Oxidation of Phenols in Water

G. N. R. Tripathi* and Yali Su

Radiation Laboratory, University of Notre Dame, Notre Dame, Indiana 46556

Received: December 31, 2003

Time-resolved Raman and transient absorption studies on hydroxyl (•OH) radical reactions with aqueous 4-carboxyphenol ($^{-}O_2C-PhOH$), the substrate in *p*-hydroxybenzoate hydroxylase, have led to the first direct observation of the basic form of a dihydroxycyclohexadienyl (•OH-adduct of phenolate anion) radical and hydration-induced intramolecular electron transfer in this species. The base-catalyzed phenoxyl radical formation in this model system has been quantitatively described in terms of pK_a of the phenolic proton (9.05) of the •OH-adduct and the rate of OH^- elimination ($2.9 \times 10^6\ s^{-1}$) from its basic form. A small fraction, 12(+2)%, of the phenoxyl radical is formed via water elimination from the •OH-adduct at the ipso position of the hydroxyl group (rate $> 10^7 s^{-1}$). About 3% •OH addition is seen at the carboxylic ipso position in basic solutions, which produces the *p*-benzosemiquinone radical anion (rate $\sim 10^6 s^{-1}$). This work provides spectroscopic and kinetic evidence of the early chemical steps in the phenoxyl radical formation by •OH oxidation and establishes the precise relationship between the formation rate and pH. A relationship between the rates of OH^- elimination from the •OH adducts of phenolate anions and pK_a of the corresponding phenols is given.

Introduction

Phenoxyl radicals represent the intermediate state in the oxidation of phenols and reduction of quinones. They have been identified in a number of biochemical systems, such as proteins and enzymes, and are implicated in cancer and aging.[1−6] The background emission observed with certain peroxyoxalate chemiluminescence reagents has been attributed to the phenoxyl radical.[3] They are associated with anti-oxidant properties of phenols that have found medical and industrial applications. The mechanism of formation, modes of reaction, and structural properties of phenoxyl radicals have been studied extensively.[6−7] Synthetic models have been developed recently for understanding the copper−phenoxyl radical array in galactose oxidase.[4] Phenoxyl radicals display CO bonds of various strengths, which have been studied recently by time-resolved Raman and electronic structure computations.[8−10] A wide variation is seen in the redox potentials ($E°$) of phenoxyl-phenolate couples ($X\text{-}PhO^•/XPhO^-$) in aqueous solution which have been used to determine the O−H bond energy in phenols.[11]

The oxidation of phenols by the •OH radical in water has remained a topic of extensive research activity because of its environmental, chemical, and biochemical implications. In the commonly held reaction mechanism, the •OH radical reacts with phenols by addition to the ring carbon sites. Phenoxyl radicals are produced by acid/base-catalyzed loss of water from the •OH-adducts (dihydroxycyclohexadienyl radicals).[5−7] A push−pull mechanism has been proposed to explain the catalysis.[7] In this mechanism, an aqueous proton attaches to the cyclohexadienyl•-OH (•OH-adduct) in acidic solutions and pulls out a water molecule, with consequent loss of the phenolic proton. In basic solutions, the hydroxyl ion removes the phenolic proton, transferring electronic charge to the cyclohexadienyl•-OH and pushing OH^- out into solution. However, the key intermediates in the mechanism, the $•OH_2^+$-adduct to a phenol in acidic solution and the •OH-adduct to a phenolate anion in basic solutions, have never been observed. Their observation and decay properties are crucial to understanding the relationship between the rate of phenoxyl radical formation and pH.

During the course of time-resolved Raman studies of phenoxyl radicals derived from aqueous 4-carboxyphenol ($^{-}O_2C-PhOH$), the substrate in oxygen-consuming enzymes *p*-hydroxybenzoate hydroxylase,[12] the vibrational features were found to be similar to that of the unsubstituted radical ($PhO^•$), showing minor effects of $-CO_2^-$ substitution on bond properties. The reduction potential of the $^{-}O_2C-PhO^•/^{-}O_2C-PhO^-$ couple (0.90 eV) is only slightly (∼12%) higher than that of $PhO^•/PhO^-$ (0.80 eV). A weak perturbation of charge distribution in PhO^- by the $-CO_2^-$ group is also indicated by the proton dissociation constant (pK_a) of $^{-}O_2C-PhOH$ (9.35) which is comparable to that of PhOH (10).[13] Thus, the structure and chemical properties of $^{-}O_2C-PhOH$ are close to those of PhOH. However, the $-CO_2^-$ perturbation, although small, slows down the rate of OH^- elimination from the •OH-adduct of $^{-}O_2C-PhO^-$. If the rate of reaction of $X\text{-}PhO^-$ with •OH can be accelerated to the extent that it becomes faster than the rate of phenoxyl radical ($X\text{-}PhO^•$) formation, the adduct precursor of the phenoxyl radical ($X\text{-}PhO^-(OH)^•$) can be observed. This condition is achievable for $^{-}O_2C-PhOH$ due to its very high solubility in water.

We have obtained the transient absorption spectrum of an •OH-adduct of a phenolate anion for the first time, using $^{-}O_2C-PhOH$ as a model system. It is this intermediate that is mainly responsible for the phenoxyl radical ($^{-}O_2C-PhO^•$, Figure 1) formation in neutral and basic aqueous solutions. The observation of $X\text{-}PhO^-(OH)^•$ is key to understanding the early chemical steps in the •OH oxidation of aqueous phenols in basic solutions. The acid−base equilibrium between the •OH-adducts of phenol and phenolate anion in this model system has been examined and a relationship between the rate of phenoxyl radical formation and pH has been derived. The rate of OH^- elimination (k_e) from

* Corresponding author. E-mail: tripathi@hertz.rad.nd.edu.

10.1021/jp031365j CCC: $27.50
Published on Web 03/30/2004

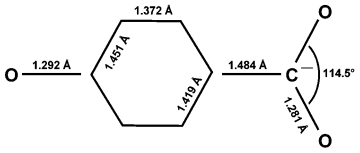

Figure 1. UB3PW91structure of $^{-}O_2C-PhO^{\bullet}$ (see text).

X-PhO^{-}(OH)$^{\bullet}$ decreases with pK_a of the phenol (X-PhOH). A relationship between the pK_a of the phenolic proton and the rate of phenoxyl radical formation has been established.

The •OH oxidation of 4-carboxyphenol has been investigated previously by transient absorption, but misassignment of the phenoxyl absorption has occurred.[14] More importantly, the •OH adduct of the phenolate anion, the key intermediate in the base-catalyzed phenoxyl radical formation, as shown in this work, was not observed.

Experimental Section

4-Carboxyphenol ($^{-}O_2C-PhOH$) was oxidized to its phenoxyl radical state in aqueous solution by pulse radiolysis. On electron pulse irradiation of N_2O-saturated water, the •OH radical is the main reactive species present in solution on the 100-ns time scale.[15] When desired, the •OH radical was converted into secondary oxidant $N_3^{\bullet}$ by reaction with 0.1 M NaN_3 in solution. Pulse radiolysis-time-resolved optical absorption and resonance Raman techniques, described in detail in several previous publications from this Laboratory, were used for transient detection.[8,16] Radiolysis by 8 MeV, 5 ns electron pulses from a linear accelerator facility in the Laboratory, which typically produces a radical concentration of 3×10^{-6} M per pulse, was used in optical absorption measurements. In Raman experiments, 2 MeV, ~100 ns electron pulses, delivered by a Van de Graaff accelerator at variable dose rates, capable of producing 5×10^{-4} M and lower radical concentrations, were applied. The Raman scattering was probed by an excimer (100 mJ)-pumped dye laser pulse (10 ns), tuned in resonance with the optical absorption of the radicals. The spectra were recorded by using an optical multichannel analyzer (OMA), accompanied with an intensified gated diode array detector, with the gate pulse synchronized with the Raman signal pulse. Extensive signal averaging was performed to improve the S/N ratio in the Raman spectra, with the accelerator and laser operated at a repetition rate of 7.5 Hz. In both experiments, a flow system was used to refresh the solution between consecutive electron pulses. Raman band positions were measured with reference to the known Raman bands of common solvents, such as ethanol, and are accurate to within ± 2 cm^{-1} for sharp bands and ± 5 cm^{-1} for broad and shoulder bands.

Results and Discussion

Spectroscopic and Structural Characterization of the Aqueous $^{-}O_2C-PhO^{\bullet}$. The transient absorption observed 2 μs after electron pulse irradiation of an N_2O-saturated aqueous solution containing 1 mM $^{-}O_2C-PhOH$ and 0.1 M NaN_3 at pH 11.3 is shown in Figure 2A. The absorption maximum (λ_{max}) is located at 415 nm ($\epsilon_{max} \sim 1650$ M^{-1} cm^{-1}), with a prominent shoulder band at 398 nm ($\epsilon_{max} \sim 1450$ M^{-1} cm^{-1}). Oxidation in this case is by $N_3^{\bullet}$ radical, which is believed to react by direct electron transfer. The reaction period, as determined by temporal evolution of optical absorption in Figure 2A, was 250($\pm$15) ns which gave a rate constant of 4.0($\pm$0.2) $\times 10^9$ M^{-1} s^{-1} for the reaction of $N_3^{\bullet}$ with $^{-}O_2C-PhO^{-}$.

The absorption spectrum in Figure 2A is different from the spectrum attributed to $^{-}O_2C-PhO^{\bullet}$ in the literature.[14] Whether

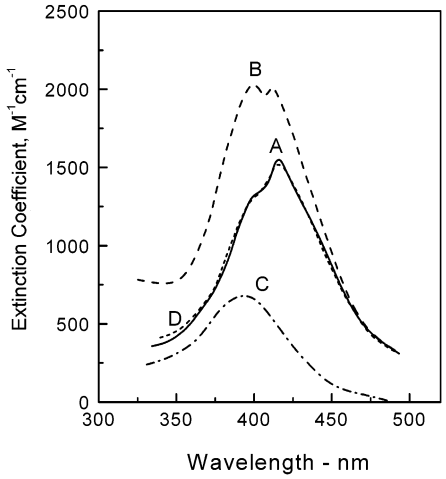

Figure 2. Transient absorption spectra obtained on electron pulse irradiation of N_2O-saturated aqueous solution containing (A) 1 mM $^{-}O_2C-PhOH$ and 0.1 M NaN_3 at pH 11.3, 1 μs after the pulse, (B) 10 mM $^{-}O_2C-PhOH$ at pH 11.2, 5 μs after electron pulse, (C) 10 mM $^{-}O_2C-PhOH$ and 0.2 M *t*-BuOH at pH 11, 5 μs after electron pulse. (D) B−C.

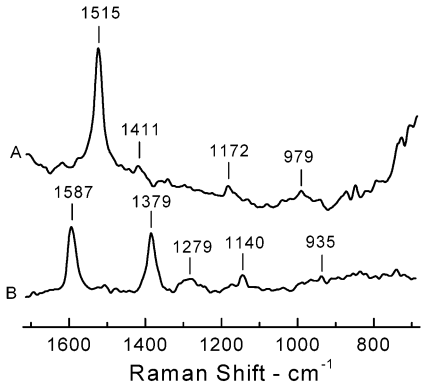

Figure 3. (A) Raman spectrum excited at 420 nm, 100 ns after electron pulse irradiation of a N_2O-saturated aqueous solution containing 5 mM $^{-}O_2C-PhOH$ and 0.1 M NaN_3 at pH 11. The transient is identified as $^{-}O_2C-PhO^{\bullet}$. (B) Raman spectrum before irradiation. Spectrum (A) is displayed after subtraction of contribution by (B) from the raw 100 ns spectrum.

the species produced by $N_3^{\bullet}$ oxidation is indeed a phenoxyl radical was ascertained by recording its resonance Raman (RR) spectra, at several excitation wavelengths between 390 and 435 nm, at different time intervals after the electron pulse. Because of low extinction coefficient, the resonance enhancement ($\propto \epsilon_{max}^2$) by the radical is relatively weak. Therefore, the spectra were recorded at the maximum permissible radiation dose rate. This is one of the rare chemical transients with $\epsilon_{max} < 2 \times 10^3$ M^{-1} cm^{-1} for which resonance Raman spectra could be obtained. Figure 3A shows the transient Raman spectrum in the 800−1700 cm^{-1} region. The spectrum was excited at 420 nm, 100 ns after the electron pulse. A strongly enhanced 1515 cm^{-1} Raman band dominates the spectrum. The spectral features are analogous to that of isoelectronic $^{-}O_2C-PhNH_2^{+\bullet}$.[17]

The intensity profiles in the 390−440 nm RR spectra of phenoxyl (X-PhO•) radicals show marked dependence on the nature of the substituent group (X).[8] The Raman spectrum in Figure 3A is typical of a phenoxyl radical that is very little affected by the nature of X. It closely resembles the RR spectra of X-PhO•, with X = H, CH_3, and F. The spectral assignment is straightforward, based on comparison with *p*-substituted phenoxyl radicals. The strong band at 1515 cm^{-1} in Figure 3A corresponds to the 1505 cm^{-1} band of PhO•, and represents the

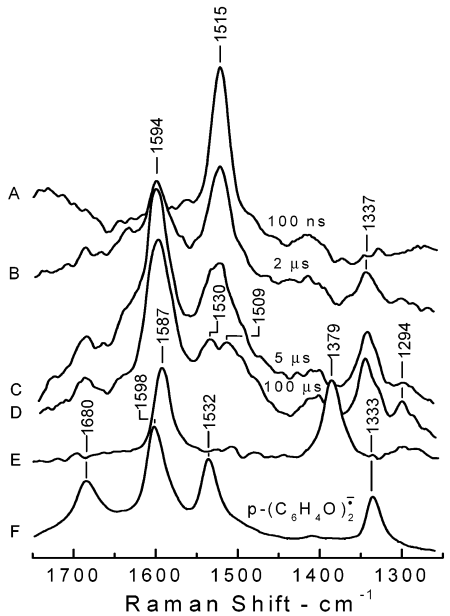

Figure 4. 435 nm Raman spectra observed on electron pulse irradiation of a N_2O-saturated aqueous solution containing 5 mM $^-O_2C-PhOH$ and 0.1 M NaN_3 at pH 11. Time-interval (A) 100 ns, (B) 2 μs, (C) 5 μs, and (D) 100 μs. (E) No electron beam. Spectra in A−D are depicted after subtraction of (E) from the raw spectra. (F) Spectrum of the *p,p′*-biphenylsemiquinone anion radical, $(OPh\text{-}PhO)^{-\bullet}$, at pH 11.

CO stretching mode. The very weak 1400 cm^{-1} band corresponds to a ring CC stretching vibration with a large CH bending component. The 1172 cm^{-1} vibration mainly involves CH bending motion and the 979 cm^{-1} vibration ring distortion. It has been shown previously that the ~980 cm^{-1} ring distortion mode is resonance-enhanced parallel to the ~1500 cm^{-1} mode.[8,9] Identification of the observed species was further supported by comparison of the experimental Raman frequencies with calculated frequencies using UHF and DFT (UB3PW91) computational procedures, details of which will be published elsewhere. The UB3PW91/6-31G** structure of the radical is furnished in Figure 1.[18]

Transient Products. The resonance Raman spectra (Figure 4) recorded at different time intervals after the electron pulse show the effect of the subsequent chemistry. The 1515 cm^{-1} $^-O_2C-PhO^\bullet$ Raman band is reduced to about half of its intensity 2 μs after the electron pulse and bands at 1594 and 1337 cm^{-1} appear (Figure 4B). At 100 μs after the electron pulse the 1515 cm^{-1} band disappears almost completely and the 1594 and 1337 cm^{-1} bands gain their maximum intensity (Figure 4D). Two weaker bands at 1530 and 1509 cm^{-1} also become apparent. Figure 4E shows Raman signals when no radiolysis was applied. These background signals (Figure 4E) have been already subtracted from the spectra in Figures 4A−D. It is known that phenoxyl radical and anisole and aniline cation radicals decay by tail−tail coupling.[17,19−21] The coupled product (4,4′-substituted biphenyl derivative) is oxidized by its radical precursor to form a radical that has an overlapping absorption and therefore is seen in resonance Raman as a transient decay product of the primary species. The mechanism of formation of the 4,4′-substituted biphenyl radicals in the reaction has been examined in detail in several previous publications from this Laboratory.[17,19,21] The coupled radical products are generally not produced when the para-position of the primary radicals is blocked by a substituent group.[17] The RR spectrum of the *p,p′*-biphenylsemiquinone anion radical $[(C_6H_4O)_2]^{-\bullet}$, produced on oxidation of 4,4′-dihydroxybiphenyl at pH 11, is displayed in Figure 4F. There is no equivalence between the Raman signals of this radical and the transient oxidation products of $^-O_2C-PhO^\bullet$ in Figure 4D. However, the spectrum in Figure 4D contains characteristic features of the radicals derived from biphenyl systems. The inter-ring stretch is observed at a frequency of ~1330 cm^{-1} in these radicals (note the presence of a band at 1337 cm^{-1} in Figure 4D).[17,19,21] The ortho and para carbon sites have high spin density in phenoxyl and its isoelectronic radicals. In para-substituted radicals, it is the ortho−ortho coupled product that is obtained.[19] We tentatively assign the spectrum in Figure 4D to 2,2′-$(^-O_2C-PhO)_2^{-\bullet}$.

It should be mentioned that $^-O_2C-PhNH_2^{+\bullet}$ is an exception to the radicals derived from para-substituted benzenes in which the tail−tail coupled radical product (benzidine cation radical) has been observed in mildly acidic solutions.[17] It is a consequence of slow decarboxylation of $^-O_2C-PhNH_2^{+\bullet}$ on the 100 μs time-scale. $^-O_2C-PhNH_2^{+\bullet}$ is isoelectronic with $^-O_2C-PhO^\bullet$. However, no evidence of decarboxylation of $^-O_2C-PhO^\bullet$ was found.

The Mechanism of the $^\bullet$OH Oxidation of Aqueous $^-O_2C-PhOH$. *Yield of Phenoxyl Radical.* Figure 2B depicts the absorption spectrum obtained on pulse radiolysis of an N_2O-saturated aqueous solution containing 10 mM $^-O_2C-PhOH$ at pH 11.2, 5 μs after the electron pulse. Under the chemical conditions used, this spectrum should mainly contain contributions from the transients produced by $^\bullet$OH oxidation. Compared to the spectrum in Figure 2A, produced by the reaction of $N_3^\bullet$ with $^-O_2C-PhO^-$, the spectrum in Figure 2B looks different. In particular, there is a prominent absorption peak at ~400 nm in Figure 2B that is not seen in Figure 2A. To determine if the transient spectrum in Figure 2B is indeed due to the $^\bullet$OH reaction, 0.2 M *tert*-butyl alcohol was added to the solution to scavenge the $^\bullet$OH radical. The spectrum obtained on radiolysis of this solution, 5 μs after the electron pulse, is shown in Figure 2C. This spectrum is tentatively attributed to the H$^\bullet$ atom adduct ($^-O_2C-PhO^-(H^\bullet)$). In $N_3^\bullet$ oxidation, the H$^\bullet$ atom is completely scavenged by N_3^- because of its high concentration in solution[22] and the $^-O_2C-PhO^-(H)^\bullet$ species is not formed. Figure 2D is the difference spectrum of Figures 2B and 2C. There is no difference in the absorption spectra in Figures 2A and 2D. The 400 nm transient was attributed previously to $^-O_2C-PhO^\bullet$.[14]

Further identification of the transient represented by the absorption in Figure 2D was done by time-resolved resonance Raman. Figure 5 shows the transient Raman spectra in the 1300−1800 cm^{-1} region, at different time intervals after the electron pulse. The RR spectrum in Figure 5A is identical to the one obtained on $N_3^\bullet$ oxidation and given in Figure 4A, except for an additional very weak Raman peak at 1620 cm^{-1}. The Raman signal intensity of $^-O_2C-PhO^\bullet$, produced by $^\bullet$OH oxidation, was comparable to that of the radical produced by $N_3^\bullet$ oxidation of $^-O_2C-PhOH$, within experimental uncertainly (±10%),[23] suggesting comparable yield of phenoxyl radical in both reactions.

In near neutral solutions a small amount of phenoxyl radical is formed at a fast rate (<100 ns). Figure 6A depicts the resonance Raman spectrum obtained on pulse radiolysis of an N_2O-saturated aqueous solution containing 5 mM $^-O_2C-PhOH$ at pH 7 (5 mM phosphate buffer), 1 μs after the electron pulse. The signal intensity is only 12% of the intensity seen on $N_3^\bullet$ oxidation (Figure 6B). We attribute this yield to the water loss from the $^\bullet$OH adduct at the ipso position to the hydroxyl group, although it may have some contribution from the hydrogen atom abstraction or direct electron transfer. It should be noted that the yield of the ipso adduct determined here by the Raman method has considerable uncertainly due to the baseline problem

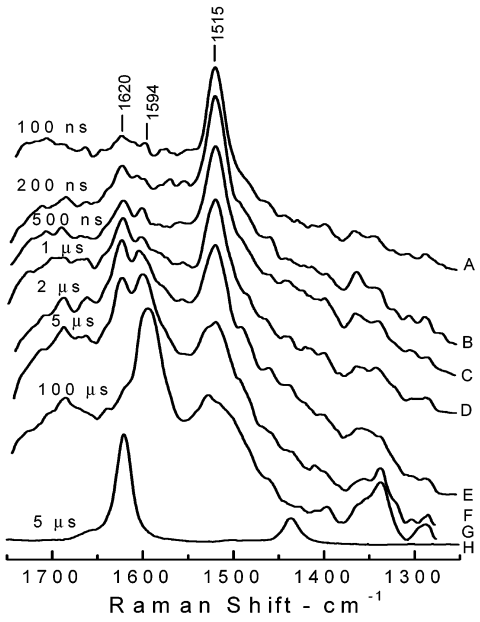

Figure 5. Raman spectra excited at 435 nm and observed (A) 100 ns, (B) 200 ns, (C) 500 ns, (D) 1 μs, (E) 2 μs, (F) 5 μs, and (G) 100 μs after electron pulse irradiation of a N_2O-saturated aqueous solution of 5 mM $^-O_2C-PhOH$ at pH 10.7. (H) 435 nm Raman spectrum of *p*-benzosemiquinone radical anion produced on electron pulse irradiation of N_2O-saturated aqueous solution of 5 mM hydroquinone at pH 11.

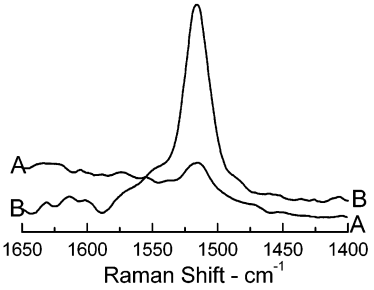

Figure 6. Raman spectrum excited at 420 nm, 100 ns after electron pulse irradiation of a N_2O-saturated solution of 5 mM $^-O_2C-PhOH$ containing (A) 5 mM phosphate buffer at pH 7 and (B). 0.1 M NaN_3 at pH 10.8.

in Figure 6A. The remaining ~88% of the •OH addition must occur at ortho, meta, and para ring positions of the hydroxyl group in $^-O_2C-PhOH$. The •OH attack at the meta positions of phenols is generally small. The meta isomer of the adduct radical is also relatively long-lived. The yield of the meta isomer has been estimated as 12% of the total •OH yield by ESR.[24] Therefore ~76% of the •OH radicals must add at the ortho and para positions, combined.

Yield of p-Benzosemiquinone Radical Anion. The weak Raman signal at 1620 cm^{-1} in Figure 5A, that is not present in the spectrum of $^-O_2C-PhO^•$ in Figure 3A, was identified with the *p*-benzosemiquinone radical anion, by comparison with the 435 nm RR spectrum obtained on oxidation of hydroquinone by •OH in basic aqueous solution (Figure 5H).[8,9,25] The maximum yield of the radical, determined by comparison with the latter spectrum, was estimated as ~3%. This signal grows at the rate of ~10^6 s^{-1} and decays on the 100 μs time scale (Figures 7A,B,C). This is a minor product of the reaction. The Raman detection of the *p*-benzosemiquinone radical anion in the •OH oxidation of several para-substituted phenols and the mechanism of formation have been discussed previously.[8] We conclude that about 73% of the •OH radicals add to the ortho position of $^-O_2C-PhO^-$.

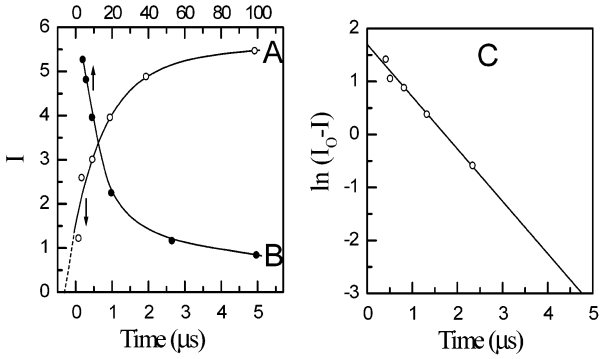

Figure 7. The growth (A) and decay (B) of the *p*-benzosemiquinone radical anion signal with time, on electron pulse irradiation of N_2O-saturated aqueous solution of 5 mM $HO_2C-PhOH$ at pH 11. (C) Plot of $\ln(I_0 - I)$ vs time. I is Raman signal intensity at time t and I_0 maximum Raman signal intensity of *p*-benzosemiquinone radical anion, monitored by the 1620 cm^{-1} peak.

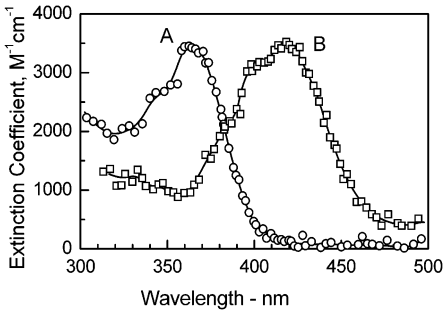

Figure 8. Absorption spectra obtained on electron pulse irradiation of a N_2O-saturated aqueous solution containing 10 mM $^-O_2C-PhOH$ and 5 mM phosphate buffer at (A) pH 7, 2.0 μs after the pulse, and (B) pH 11, 100 ns after the pulse.

The Adduct Precursors. The absorption spectra of numerous •OH-adducts of phenols are reported in the literature, with λ_{max} in the 360 nm region.[5−7] These transients decay by reaction with base to form the phenoxyl radical. On electron pulse radiolysis of N_2O-saturated aqueous $^-O_2C-PhOH$ at pH ~ 7 (phosphate buffer), a transient absorption at 365 nm (λ_{max}) appears as the initial reaction product which we attribute mainly to the •OH adduct of $^-O_2C-PhOH$ at the ortho position (Figure 8A). From the rate of formation of this species, the rate constant for the reaction of •OH with $^-O_2C-PhOH$ was determined as $6(\pm1) \times 10^9$ M^{-1} s^{-1}. We have estimated that about 73(±10)% of the •OH radicals add to the ortho position. There is a drop in the yield of the 365 nm transient with pH (Figure 9), indicating that this species is in equilibrium with another species, which is a likely precursor of the phenoxyl radical. This precursor species can be readily observed if its rate of formation is faster than that of the phenoxyl radical. This condition is satisfied with a high concentration (>5 mM) of $^-O_2C-PhOH$ in solution.

A high concentration of $^-O_2C-PhOH$ shortens the reaction period with •OH and catalyzes the acid−base equilibrium of the •OH adduct (this catalysis is briefly discussed below). In the pH range 7−10, OH^- concentration in solution is too low to induce equilibrium on the sub-microsecond or a shorter time scale. Considering a diffusion-controlled limit for the rate of reaction of the •OH adduct with the parent phenol, at least a 10 mM concentration of $^-O_2C-PhOH$ is required to attain acid−base equilibrium on the 10 ns time scale. A high substrate concentration is key to observing the •OH adduct of a phenolate anion and following its decay into the phenoxyl radical.

The absorption spectrum of the transient produced on reaction of •OH with 10mM $^-O_2C-PhOH$ at pH 11 is shown in Figure

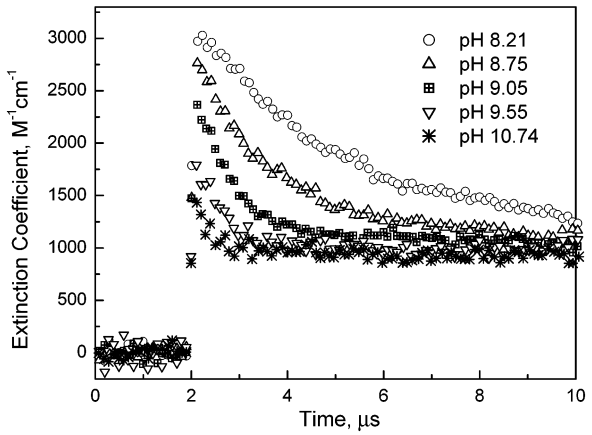

Figure 9. Time dependence of the 365 nm absorption at pH 8.21, 8.75, 9.05, 9.55, and 10.74 for N_2O-saturated aqueous solution of 10 mM $^-O_2C-PhOH$ with 5 mM phosphate buffer.

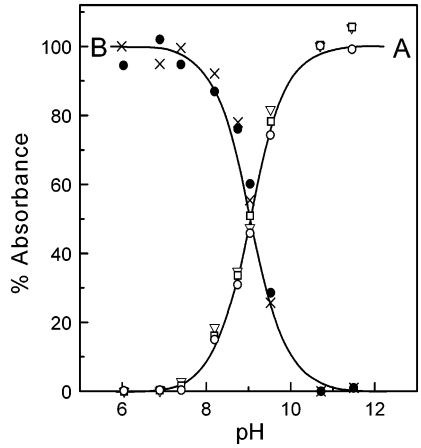

Figure 10. pH dependence of the percentage initial absorbance of (A) 365 nm transient and (B) 420 nm transient, measured at different wavelengths, after electron pulse irradiation of N_2O-saturated aqueous solution containing 10 mM $^-O_2C-PhOH$ and 5 mM phosphate buffer. pK_a of the •OH adduct determined as 9.05 (±0.05) from the acid−base titration curve.

8B. The λ_{max} in this spectrum is similar to that of $^-O_2C-PhO^•$ (Figure 2A), but ϵ_{max} is about twice as large at 420 nm. The initial (~30 ns) absorbance of the 420 and 365 nm transients monitored with pH is shown in Figure 10. It can be seen that the two species interconvert with change in pH. There is little doubt that the 365 and 420 nm transients (Figure 8) represent the acid and basic forms of the same species. The pK_a of the species is determined as 9.05 from Figure 10. If the acid−base equilibrium is not established, for which a high substrate concentration in solution is required, the pH-dependence of the 365 nm absorbance will give a false pK_a. Also, the rate of phenoxyl radical formation from the basic form of the •OH adduct cannot be correctly estimated. To our knowledge, no earlier report on the acid−base equilibrium of the •OH adduct of a phenol, as presented in Figure 10, can be found in the literature.

Intramolecular Electron Transfer and Phenoxyl Radical Formation. The mechanism of phenoxyl radical formation becomes quite clear as one monitors the rate of decay of the •OH adducts and formation rate of the phenoxyl radical (Figures 9 and 11). As $^-O_2C-PhO^•$ and its adduct precursor have overlapping and rather similar absorptions (Figures 2B and 8B), it would be difficult to make a distinction between them, particularly if they had comparable absorbance, unless resonance Raman spectroscopy is applied as a diagnostic tool. At pH >

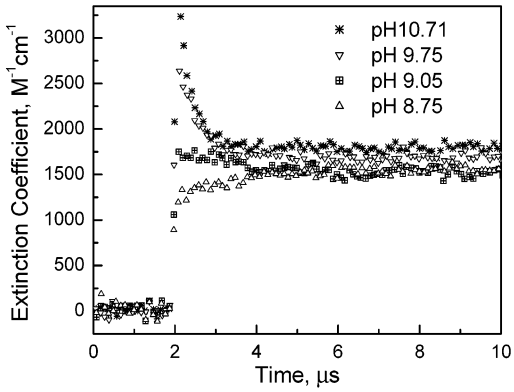

Figure 11. Time dependence of absorption at 420 nm at pH 10.74, 9.55, 9.05, and 8.75 for N_2O-saturated solution of 10 mM $^-O_2C-PhOH$ and 5 mM phosphate buffer. There is no change in absorbance with time at pH 9.05, as decay of absorption due to the •OH adduct of $^-O_2C-PhO^-$ is compensated by the growth of absorption due to the phenoxy radical $(^-O_2C-PhO)^•$. The extinction coefficient of the later radical is half of its precursor at 420 nm.

11, the OH-adduct of $^-O_2C-PhO^-$ (420 nm transient, Figure 8B) decays at a rate of 2.9×10^6 s^{-1} ($t_{1/2} = 0.24$ μs), and this rate is independent of pH. As pointed out earlier, time-resolved Raman positively identifies the species formed on decay of the •OH-adduct as the phenoxyl radical. The rate of OH^- loss from $^-O_2C-PhO^-(OH)^•$ ($k_e = 2.9 \times 10^6$ s^{-1}) is an order of magnitude faster than the rate of OH^--elimination from the •OH adduct of $^-O_2C-PhNH_2$.[17] However, the rate of OH^- elimination from the protonated form, $^-O_2C-PhOH(OH)^•$, is much slower (see later sections). The amine group behavior is intermediate between that of O^- and OH in this respect.

The pH-Dependence of Phenoxyl Radical Formation. The acid−base equilibria of the parent phenols occurs in the same pH range as that of the •OH adducts. The rate constant for the reaction of •OH is usually identical for both forms of phenols. If the rate of phenoxyl radical formation from the basic form of phenol were faster than that from the acid form, the observed rate would show pH-dependence, even if the •OH did not add to phenolate. However, the decay of $^-O_2C-PhOH(OH)^•$ would not correspond with the growth of the phenoxyl radical that is commonly observed.

With the observation of $^-O_2C-PhO^-(OH)^•$ and its rate of conversion into phenoxyl radical, a precise relationship between the rate of phenoxyl radical formation and pH can be worked out. Let us consider the acid−base equilibrium of the •OH adduct and phenoxyl formation, as shown below:

$$^-O_2C\text{-}PhOH(OH)^• + B^- \underset{k_r}{\overset{k_f}{\rightleftharpoons}} {}^-O_2C\text{-}PhO^-(OH)^• + BH \qquad (1)$$

$$\downarrow k_e$$

$$^-O_2C\text{-}PhO^• + OH^-$$

B is the total base concentration in solution. Equilibrium (1) will be reached only when $k_r + k_f \gg k_e$.[26] The rate (k) of phenoxyl ($^-O_2C-PhO^•$) radical formation is given by

$$k = k_e k_f/(k_r + k_f) \qquad (2)$$

where $k_f/(k_r + k_f)$ is the fraction of the basic form of the •OH adduct at a particular pH of solution which can be estimated from Figure 10. The solid line in Figure 10A represents a theoretical expression for the equilibrium fraction $\{(k_f/(k_r + k_f)\}$ of $^-O_2C-PhO^-(OH)^•$, given by $10^{(pH-pK_a)}/(1 + 10^{(pH-pK_a)})$,

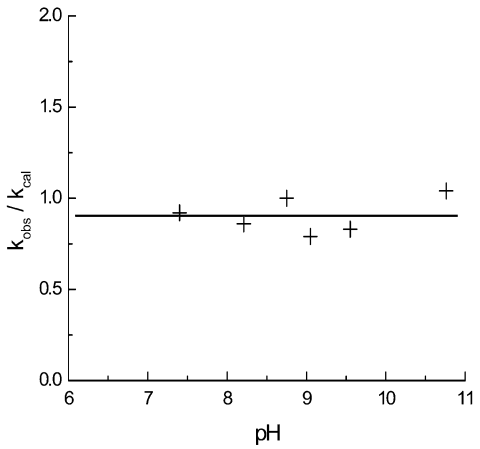

Figure 12. Comparison between observed (k_{obs}) and calculated (k_{cal}) rates of the phenoxyl radical formation at different pH levels.

and the solid line in Figure 10B that of $^{-}O_2C-PhOH(OH)^{\bullet}$ (k_f / (k_r + k_f)), given by $1/(1 + 10^{(pH-pK_a)})$. The observed and calculated values of k for different pH levels are compared in Figure 12. It can be seen that there is an excellent agreement between the experimental and theoretical values of k. If a similar behavior is assumed for all phenols, the only parameters that are needed for quantitative estimation of the rate of phenoxyl radical formation (k) are the pK_a of X-PhOH(OH)• and k_e.[27]

As pointed out earlier, the equilibrium (1) is catalyzed by the substrate. At pH < 9 ($k_f \ll k_r$), k can be approximated as (k_f /k_r) k_e. The decay rate of the 365 nm transient, monitored at pH 8.4, was found to increase almost linearly with the $^{-}O_2C-PhOH$ concentration (between 1 mM and 10 mM) in solution, according to the relation, k (s^{-1}) = $7.5 \times 10^4 + 2.8 \times 10^8[^{-}O_2C-PhO^{-}]$. This dependence suggests that the rate constant for the reaction of $^{-}O_2C-PhOH(OH)^{\bullet}$ with $^{-}O_2C-PhO^{-}$ is slower than the rate constant for the reaction of $^{-}O_2C-PhO^{-}(OH)^{\bullet}$ with $^{-}O_2C-PhOH$, which we estimate as $\geq 10^9$ M^{-1} s^{-1} and $\geq 1.5 \times 10^9$ M^{-1} s^{-1}, respectively. The term 7.5×10^4 s^{-1} in k combines the rates of OH^{-}-induced and spontaneous loss of water from $^{-}O_2C-PhOH(OH)^{\bullet}$, which we roughly estimate as 1.5×10^4 s^{-1} and 6×10^4 s^{-1}, considering that OH^{-} should react at a diffusion-controlled rate.

The decay kinetics of $^{-}O_2C-PhO^{-}(OH)^{\bullet}$ transient (420 nm) and its conversion into the phenoxyl radical is shown in Figure 11. It can be seen that the excess absorption at 420 nm decays at a slower rate with decrease in pH, determined by the fraction of adduct to phenolate at ~30 ns. At pH 9.05, there is no change in absorbance with time, as the drop in the absorbance of the adduct radical due to its decay into the phenoxyl radical is compensated by the growth of absorbance of the phenoxyl radical. At pH 8.75, there is a slight growth of absorbance at 420 nm, as the $^{-}O_2C-PhO^{-}(OH)^{\bullet}$ absorption at ~30 ns is less than the absorption of the phenoxyl radical into which it decays.

Relationship between pK_a of the •OH Adduct and k_e. Trends in the data available in the literature indicate that the rate of phenoxyl radical formation from the •OH adduct of a phenolate anion (k_e) depends on pK_a of its acid form. If pK_a is too low, as in nitrophenols, formation of the phenoxyl radical is not observed. Unfortunately, the pK_a values of phenolic protons in the •OH adducts are not known. Therefore we assume that they are comparable to or slightly lower (~0.3 eV) than pK_a values of the parent phenol, in view of the results obtained in this work.

The pK_a values of the hydroxycyclohexadienyl radicals are similar to those of the hydroxyl proton in aliphatic alcohols or water (p$K_a \sim 15$).[28] In other words, the added OH group is not part of the conjugated system. Therefore, one can safely assume minimal dependence of the ring-OH bonding in the •OH adduct (X-$PhO^{-}(OH)^{\bullet}$) and its transition state (X-$PhO^{\bullet}(OH^{-})$) on the nature of X-PhO^{-}. On the other hand the negative charge on O is delocalized in X-PhO^{-}, which amounts to structural stabilization by a free energy (ΔG° in eV) difference of $0.059 \times \Delta pK_a$, with respect to a hypothetical reference system ($\Delta pK_a = 0$) for which there is no delocalization of the charge.[29] ΔG° is additional energy required to attain the transition state (X-PhO^{-}-$(OH)^{\bullet} \rightarrow$ X-$PhO^{\bullet}(OH^{-})$), and is expected to lower the rate of OH^{-} elimination by a factor of $\exp(-\Delta G^{\circ}/RT)$. In other words, $k_e = k_0 \exp(-\Delta G^{\circ}/RT)$, where k_0 is a constant that relates to the reference system (e.g., pK_a = 15).[29,30] Using $k_e = 2.9 \times 10^6$ s^{-1}, pK_a = 9.05 and $\Delta pK_a = 5.95$ for $^{-}O_2C-PhOH(OH)^{\bullet}$, we estimate $k_0 = 2.5 \times 10^{12}$ s^{-1}. Since pK_a for any other •OH adduct (X-$PhOH(OH)^{\bullet}$) is not yet known, it is useful to relate k_e to pK_a of the parent phenol (X-PhOH), which is 0.3 eV higher than that of the •OH adduct for X = $^{-}O_2C$. Thus, we use $k_e = k_0' \exp(-\Delta G^{\circ}/RT)$, where $k_0' = k_0 \exp(-0.3 \times 0.059/RT) = 1.25 \times 10^{12}$ s^{-1}, and ΔG° (in eV) = $0.059 \times \Delta pK_a$ for the phenol, for estimation of k_e in different systems.

TABLE 1: Observed and Estimated Rates of Decay of •OH Adducts to Phenolate Anions Forming Phenoxyl Radical (X-$PhO^{-}(OH)^{\bullet} \rightarrow$ X-$PhO^{\bullet} + OH^{-}$) in Basic Aqueous Solutions

phenol (XC_6H_4OH)	pK_a[a]	rate of phenoxyl radical formation (k_e)	
		k_{cal}	k_{obs}
X = CO_2^{-}	9.35 (9.05)[b]	2.9×10^6	2.9×10^6
X = $COCH_3$	8.79	7.7×10^5	7×10^5
X = CHO	[c]		4×10^5
X = CN	8.3	2.5×10^5	3×10^5
X = NO_2	7.05	7×10^4	7×10^5
X = H	9.9	10^8	$>10^7$

[a] pK_a of phenols (XPhOH). [b] pK_a of •OH adduct (X$PhOH(OH)^{\bullet}$). [c] Estimated pK_a= 8.69, assuming $k_{cal} = k_{obs}$.

The estimated decay rates of the •OH adducts forming phenoxyl radical ((X-$PhO^{-}(OH)^{\bullet} \rightarrow$ X-$PhO^{\bullet} + OH^{-}$) are given in Table 1 for a few selected phenolates. Experimental determination of k_e has been made for X = CN, CHO, and $COCH_3$ in *p*-X-PhOH by conductivity method.[7] For X = CN (pK_a = 8.3), estimated $k_e = 2.5 \times 10^5$ s^{-1} and observed $k_e = 3 \times 10^5$ s^{-1}. For X = $COCH_3$ (pK_a = 8.79), estimated $k_e = 7.7 \times 10^5$ s^{-1} and observed $k_e = 7 \times 10^5$ s^{-1}. It can be seen that there is an excellent agreement between the estimated k_e and the observed k_e for the systems for which experimental data is available. pK_a for X = CHO could not be found in the literature. For X = NO_2, pK_a = 7.05 and estimated $k_e = 1.4 \times 10^4$ s^{-1}. This rate is quite low and the formation of phenoxyl radical is unlikely to be observed due to interference of radical−radical reactions, unless the experiments are performed at initial radical concentration of $\sim 10^{-6}$ M or less. For unsubstituted phenoxyl (X = H), pK_a = 9.9 and the estimated $k_e \sim 10^8$ s^{-1}. Therefore, the •OH adduct to phenolate anion is potentially observable, if experiments are performed at a substrate concentration of >100 mM. To our knowledge, the reaction of hydroxyl radical with high concentrations of aqueous phenols has not yet been investigated.

Summary

The structure and functions of phenoxyl radicals in proteins and enzymes and DNA interactions in biochemical systems are of current scientific interest. The reaction of hydroxyl radical

(•OH) with organic substrates is of fundamental importance in environmental chemistry, synthetic organic chemistry, and radiation biology. This paper presents a mechanistic investigation of the hydroxyl radical reaction with phenols, using 4-carboxyphenol as a model system. The •OH adduct of a phenolate anion, which is a key intermediate in the phenoxyl radical formation, has been observed for the first time and its acid−base equilibrium has been examined. The adduct radical decays into phenoxyl radical, identified by time-resolved resonance Raman spectroscopy.

Two important relationships that define the early chemical events in the •OH oxidation of phenols in water have been developed. The first is concerned with the relationship between the rate of phenoxyl radical formation (k) and base concentration in solution, and the second is concerned with the dependence of k on pK_a of phenols. $k = k_e \times 10^{(pH-pK_a)}/(1 + 10^{(pH-pK_a)})$, where k_e is the spontaneous decay rate of the •OH adduct of the phenolate anion and pK_a relates to its acid form. k_e and pK_a in different phenolates relate by $k_e = k_0 \exp(-0.059 \times \Delta pK_a/RT)$, where ΔpK_a is estimated with respect to an aliphatic reference system for which pK_a = 15. The value of k_0 is estimated as 1.25×10^{12} s^{-1}, if pK_a of the parent phenol is used for determination of k_e, and as 2.5×10^{12} if the pK_a of the •OH adduct is used. This relationship has been applied to phenols for which values of k_e are known and an excellent agreement has been found.

Acknowledgment. The research described herein was supported by the Office of Basic Energy Sciences of the Department of Energy. This is Contribution No. NDRL 4407 from the Notre Dame Radiation Laboratory.

References and Notes

(1) Lucarini, M.; Mugnaini, V.; Pedulli, G. F.; Guerra, M. J. *J. Am. Chem. Soc.* **2003**, *125*, 8318.

(2) Barnett, N. W.; Hindson, B. J.; Lewis, S. W. *Anal. Chim. Acta* **1998**, *362*, 131. Nordlund, P.; Sjoberg, B.-M.; Eklund, H. *Nature* **1990**, *345*, 593. Bender, C. J.; Sahlin, M.; Babcock, G. T.; Barry, B. A.; Chandrashekar, T. K.; Salowe, S. P.; Stubbe, J.; Lindstrom, B.; Petersson, L.; Ehrenberg, A.; Sjoberg, B.-M. *J. Am. Chem. Soc.* **1989**, *111*, 2245. Babcock, G. T. *Proc. Natl. Acad. Sci. U.S.A.* **1993**, *90*, 10893, and references therein. Xie, C.; Lahti, P. M. *Tetrahedron Lett.* **1999**, *40*, 4305−4308.

(3) Barnett, N. W.; Bos, R.; Lewis, S. W.; Russell, R. A. *Anal. Commun.* **1997**, *34*, 17.

(4) Halfen, J. A.; Jazdzewski, B. A.; Mahapatra, S.; Berreau, L. M.; Wilkinson, E. C.; Que, L., Jr.; Tolman, W. B. *J. Am. Chem. Soc.* **1997**, *119*, 8217. Jazdzewski, B. A.; Tolman, W. B. *Coord. Chem. Rev.* **2000**, *200*, 633.

(5) von Sonntag, C. *The Chemical Basis of Radiation Biology*; Taylor and Francis: New York, 1987.

(6) Land, E. J.; Ebert, M. *Trans. Faraday Soc.* **1967**, *63*, 1181. Raghavan, N. V.; Steenken, S. *J. Am. Chem. Soc.* **1980**, *102*, 3495. Mvula, E.; Schuchmann, M. N.; von Sonntag, C. *J. Chem. Soc., Perkin Trans. 2* **2001**, 264.

(7) Steenken, S. *Top. Curr. Chem.* **1996**, *177*, 125. Steenken, S. *J. Chem. Soc., Faraday Trans., 1* **1987**, *83*, 113, and references therein.

(8) Tripathi, G. N. R. In *Advances in Spectroscopy, Vol. 18, Time-resolved Spectroscopy*; Clark, R. J. H., Hester, R. E., Eds.; John Wiley & Sons: New York, 1989; pp 157−218.

(9) Tripathi, G. N. R. *J. Chem. Phys.* **2003**, *118*, 1378. Tripathi, G. N. R. *J. Phys. Chem. A* **1998**, *74*, 6044; *J. Am. Chem. Soc.* **1998**, *120*, 5134. Tripathi, G. N. R.; Sun, Q.; Schuler, R. H. *Chem. Phys. Lett.* **1989**, *156*, 51. Tripathi, G. N. R.; Schuler, R. H. *J. Phys. Chem.* **1987**, *91*, 5881. Tripathi, G. N. R.; Schuler, R. H. *J. Phys. Chem.* **1988**, *92*, 5129. Sun, Q.; Tripathi, G. N. R.; Schuler, R. H. *J. Phys. Chem.* **1990**, *94*, 6273. Tripathi, G. N. R.; Schuler, R. H. *J. Chem. Soc., Faraday Trans.* **1993**, *89*, 4177. Mukherjee, A.; McGlashen, Z.; Spiro, T. G. *J. Phys. Chem.* **1995**, *99*, 4912. For earlier references, see citations in ref 6.

(10) Engström FS, M.; Himo, F.; Gräslund, A.; Minaev, B.; Vahtras, O.; Ågren, H. *J. Phys. Chem. A* **2000**, *104*, 5149. Wise, K. E.; Pate, J. B.; Wheeler, R. A. *J. Phys. Chem. B* **1999**, 4764. Chipman, D. M.; Liu, R.; Zhou, X.; Pulay, P. *J. Chem. Phys.* **1994**, *116*, 44, and references therein.

(11) Das, T. N.; Neta, P. *J. Phys. Chem. A* **1998**, *102*, 7081. Lind, J.; Shen, X.; Eriksen, T. E.; Merényi, G. *J. Am. Chem. Soc.* **1990**, *112*, 479, and references therein.

(12) Eppink, M. H.; Bunthol, C.; Schreuder, H. A.; van Berkel, W. J. *FEBS Lett.* **1999**, *443*, 251. Eppink, M. H.; Schreuder, H. A.; van Berkel, W. J. *Eur. J. Biochem.* **1995**, *231*, 157. van Berkel, W.; Westphal, A.; Eppink, M.; de Kok, A. *Eur. J. Biochem.* **1992**, *201*, 411, and references cited in these papers.

(13) Serjeant, E. P.; Dempsey, P. *Ionization Constants of Organic Acids in Aqueous Solution*; Pergamon Press: Oxford, 1979.

(14) Anderson, R. F.; Patel, K. B.; Stratford, M. R. L. *J. Chem. Soc., Faraday Trans.* **1987**, *83*, 3177.

(15) Buxton, G. V.; Greenstock, C. L.; Helman, W. P.; Ross, A. B. *J. Phys. Chem. Ref. Data* **1988**, *17*, 513.

(16) Tripathi, G. N. R. In *Multichannel Image Detectors II*; Talmi, Y., Ed.; ACS Symposium Series 236; American Chemical Society: Washington, DC, 1983; p 171. Patterson, L. K.; Lilie, J. *Int. J. Radiat. Phys. Chem.* **1974**, *6*, 129. Janata, E.; Schuler, R. H. *J. Phys. Chem.* **1982**, *86*, 2078.

(17) Tripathi, G. N. R.; Su, Y. *J. Am. Chem. Soc.* **1996**, *118*, 2235.

(18) Tripathi, G. N. R., unpublished results. Calculated frequencies 1502, 1449, 1162, and 983 cm^{-1} match well with the experimental frequencies.

(19) Tripathi, G. N. R. *Chem. Phys. Lett.* **1992**, *409*, 199.

(20) Nonhebel, D. C.; Walton, J. C. *Free-radical Chemistry: Structure and Mechanism*; Cambridge University Press: New York, 1974.

(21) Tripathi, G. N. R.; Schuler, R. H. *Radiat. Phys. Chem.* **1988**, *32*, 251. Tripathi, G. N. R.; Chipman, D. M. *J. Phys. Chem. A* **2002**, *106*, 8908.

(22) Alfassi, Z. B.; Schuler, R. H. *J. Phys. Chem.* **1985**, *89*, 3359.

(23) The yield of N_3• is 10% higher than that of •OH, which is within the uncertainty of the yield measured by weak Raman signals.

(24) Neta, P.; Fessenden, R. W. *J. Phys. Chem.* **1974**, *78*, 523.

(25) Tripathi, G. N. R. *J. Am. Chem Soc.* **2003**, *125*, 1178, and references therein.

(26) Bell, R. P. *The Proton in Chemistry*; Cornell University Press: Ithaca, New York, 1959.

(27) In the case of the rate of reaction of •OH with phenol $\ll k_e$, the formation of phenoxyl radical from phenolate anion would appear to occur at a diffusion-controlled rate and no distinction can be made between the base-catalyzed loss of water from the •OH adduct of neutral phenol and the loss of H^+ and OH^- in two successive steps from this species as demonstrated here.

(28) Taniguchi, H.; Schuler, R. H. *J. Phys. Chem.* **1985**, *89*, 3095; *J. Am. Chem. Soc.* **1984**, *106*, 1507.

(29) Pauling, L. *The Nature of the Chemical Bond*; Cornell University Press: Ithaca, New York, 1960.

(30) The pK_a of the reference system is taken as 15 for illustration, and the value of k_0 depends on this choice. However, the relationship between the rate of decay of the •OH adduct of the phenolate anion and pK_a of the corresponding phenol is independent of this choice.